# New Elements Concentrated Planar Fractal Antenna Arrays for Celestial Surveillance and Wireless Communications

Ahmed Najah Jabbar

**This research introduces three new fractal array configurations that have superior performance over the well-known Sierpinski fractal array. These arrays are based on the fractal shapes Dragon, Twig, and a new shape which will be called Flap fractal. Their superiority comes from the low side lobe level and/or the wide angle between the main lobe and the side lobes, which improves the signal-to-intersymbol interference and signal-to-noise ratio. Their performance is compared to the known array configurations: uniform, random, and Sierpinski fractal arrays.**

**Keywords: Fractals, antenna array, random array, uniform array, planar array, fractal array, phased antenna arrays.**

Manuscript received Jan. 21, 2011; revised Apr. 3, 2011; accepted Apr. 18, 2011.

Ahmed Najah Jabbar (phone: +96 47808249099, email: Ahmed_AlJafari@yahoo.com) is with the Electric Department, College of Engineering, University of Babylon, Hilla, Babylon, Iraq.

http://dx.doi.org/10.4218/etrij.11.0111.0036

## I. Introduction

The performance of any wireless system depends heavily on the antenna section. The antenna is responsible for collecting the transmitted information and directs it to the next stage. Hence, careful design of the antenna ensures stable and reliable RF signal flow.

Antenna arrays are widely used in modern communication systems to enhance the directivity, electronic scanning, and steering the main beam to track a source [1], [2]. The easiest way to arrange antennas within an array is to use the uniform antenna array (UAA). In UAA, the antennas are spaced by a fixed distance depending on the wavelength $\lambda$ [3], [4]. The array factor (AF) is directly related to the number of antennas and the spacing between them. Although this arrangement is commonly used, its AF depends heavily on the topology: hence, they lack robustness in hostile environments [5]. To overcome the dependence on the topology, random antenna array (RAA) was introduced. In this array, the antennas are placed randomly. While this arrangement was able overcome dependence of the AF on the array topology, it suffers from the high side lobe level (SLL) [6].

Fractals were introduced by B.B. Mandelbrot during 1970's. The fascinating feature of a fractal is that it can replicate itself indefinitely without losing its original shape. The iterated function system (IFS) is a method that is used to generate fractals [7], [8]. In this method, the required generator shape is created and then iterated to create the fractal. This feature attracted the designers to develop new array topologies that are called fractal antenna arrays (FAA). These arrays cannot be

  

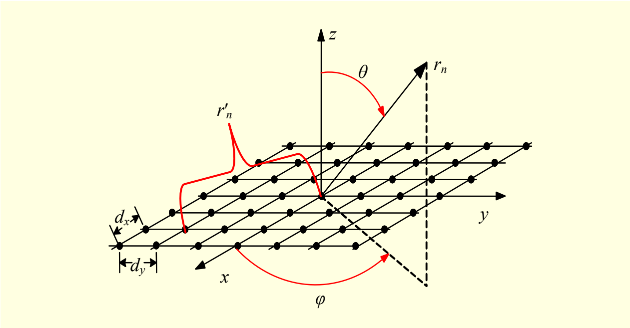


Fig. 1. Uniform planar phased array antenna.

classified as UAAs nor RAAs because fractals inherit the spacing from their predecessors and scale them down depending on the iteration level. This arrangement may inherit the low SLL of the UAA and the robustness of the RAA.

Many efforts were devoted to investigate this new trend in antenna array. Impressive studies of fractal arrays are given in [9]-[14].

FAAs found their way into many wireless communication applications [15]-[20] because of their flexibility and the property of multiple frequency tuning.

## II. Array Factor

For any phased antenna array, the radiation pattern, at the far field (*Fraunhofer*), is the multiplication of two main parts: the element radiation pattern and array factor (AF). The array factor contains the dependence on $r$, $\varphi$, and $\theta$ which are the distance, the azimuth angle, and the elevation angle, respectively, between the array and the observer. Consider the UAA shown in Fig. 1 having $N\times M$ isotropic elements along the $x$, $y$ directions.

The far electric field generated by a single element is [21], [22]

$$E_n(r) \approx -j\omega\mu \frac{\exp(-jkr)}{4\pi r} f_n(\theta,\varphi), \tag{1}$$

and the angular-dependent vector is

$$f_n(\theta,\varphi)=\left(\hat{\theta}\theta+\hat{\varphi}\varphi\right)\cdot \int_{\text{element}} J_n(r'_n)\exp\left(jk\hat{r}\cdot(r_n-r'_n)\right)d\upsilon', \tag{2}$$

where $J_n(r'_n)$ is the electric current density of the $n$-th element, $r'_n$ is the distance of the $n$-th element from the origin, $r_n$ is the distance between the observer and the origin, $k$ is the freespace wave number $2\pi/\lambda$, $\omega$ is the angular frequency, and $\mu$ is the magnetic permeability.

The total electric field for the $N\times M$ elements using superposition is

$$E(r) = \sum_{n}^{N,M} E_n(r). \tag{3}$$

For identical uniformly spaced elements, $f_n(\theta,\varphi)$ is

$$f_n(\theta,\varphi) = I_n f(\theta,\varphi), \tag{4}$$

where $I_n$ is the complex excitation of the $n$-th element and $f(\theta,\varphi)$ is the pattern function.

Combining the above equations and using the spherical coordinates, we have

$$E(r) = \overbrace{-j\omega\mu \frac{\exp(-jkr)}{4\pi r} f(\theta,\varphi)}^{\text{Element radiation pattern}} AF(\theta,\varphi), \tag{5}$$

where $AF$ is the array fctor which is

$$AF(\theta,\varphi) = \sum_{N,M} I_n(\theta,\varphi)\exp(jkr_n\cos(\xi_n)), \tag{6}$$

where $\cos(\xi_n) = \sin(\theta_n)\sin(\theta)\cos(\varphi-\varphi_n)+\cos\theta\cos\theta_n$.

The array factor is the part that is used to steer the main lobe to the required direction and to measure the directivity of the array. For UAA, if the distances are changed or elements are lost, AF will change dramatically.

## III. Fractal Arrays and Multifrequency Tuning

Mandelbrot has pointed out that fractals are bounded and seem to be the result of a favorite construction principle in nature. Mathematically, an iterated function system (IFS) is a method used for constructing fractals; the resulting fractals are always self-similar.

To define a fractal, let us start with an affine map defined as

$$\Im(\chi) := L\chi + b, \tag{7}$$

where $L$ is a linear map and $b\in\Re^2$. The above relation can be written using matrix notation as [7], [8]

$$\begin{pmatrix}\Im(\chi)_1\\ \Im(\chi)_2\end{pmatrix} = \begin{pmatrix} l_{11} & l_{12}\\ l_{21} & l_{22}\end{pmatrix}\begin{pmatrix}\chi_1\\ \chi_2\end{pmatrix} + \begin{pmatrix} b_1\\ b_2\end{pmatrix}, \tag{8}$$

where $l_{11}, l_{12}, l_{21}, l_{22}, \chi_1, \chi_2, b_1, b_2 \in \Re^2$. Using homogenous coordinates, (8) can be represented in matrix format as

$$\Im([\chi_1,\chi_2,1]) = [\chi_1,\chi_2,1]\begin{bmatrix} l_{11} & l_{21} & 0\\ l_{12} & l_{22} & 0\\ b_1 & b_2 & 1\end{bmatrix} = [\chi_1,\chi_2,1]F. \tag{9}$$

To generate an equilateral Sierpinski fractal, we let

$$\Im_1([\chi_1,\chi_2,1]) = [\chi_1,\chi_2,1]\begin{bmatrix} 0.5 & 0 & 0\\ 0 & 0.5 & 0\\ 0.25 & 0 & 1\end{bmatrix},$$

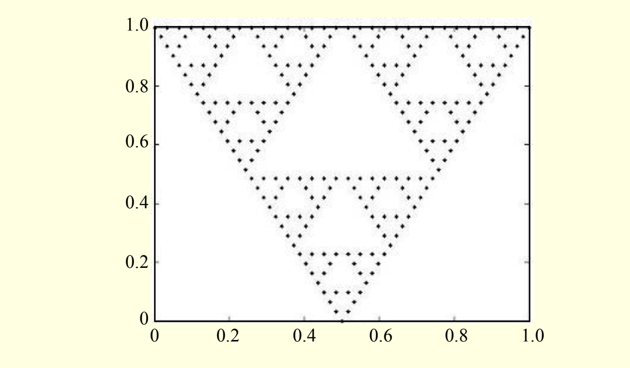


Fig. 2. Equilateral Sierpinski fractal.

$$\Im_2([\chi_1,\chi_2,1])=[\chi_1,\chi_2,1]\begin{bmatrix}0.5 & 0 & 0\\ 0 & 0.5 & 0\\ 0 & 0.5 & 1\end{bmatrix},$$

$$\Im_3([\chi_1,\chi_2,1])=[\chi_1,\chi_2,1]\begin{bmatrix}0.5 & 0 & 0\\ 0 & 0.5 & 0\\ 0.5 & 0.5 & 1\end{bmatrix}.$$

The resulting fractal is shown in Fig. 2. From Fig. 2, we can see that the distance between two points (which represent elements locations) are neither uniform nor random. At a single level, the spacings are equal but advancing to higher levels; the distances are divided by 2 for every iteration. This concept will be used to explain the principle of multifreqeuncy tuning.

In section II, (6) represents the AF for the UAA. We need to modify this equation to describe AF for the FAA as [6], [23]-[25]

$$AF_P(\psi)=\prod_{p=1}^{P} GA(\delta^{p-1}\psi), \tag{10}$$

where $p$ represents the iteration level, $\psi$=$kd\sin(\theta,\varphi)$, $\delta$ is the excitation phase scale for each element, and $GA(\psi)$ represents the generating AF.

Letting $p\rightarrow\pm\infty$ then

$$\begin{aligned} AF_P(\psi) &= \prod_{p=-\infty}^{\infty} GA\left(\delta^{\pm q-1}\psi\right) \\ &= \prod_{p=-\infty}^{\infty} GA\left(\delta^{\upsilon-1}\psi\right)=AF(\psi), \end{aligned} \tag{11}$$

with $q$ is a natural number and $\upsilon=|q|$.

From (11), we can see that the AF is scaled by $q$ factor. This scaling is analogous to scaling the tuning frequency such that $f_{\pm q}=\delta^{\pm q} f_0$.

## IV. Simulation and Results

Recalling Fig. 1 and (6) (which is in spherical coordinates),

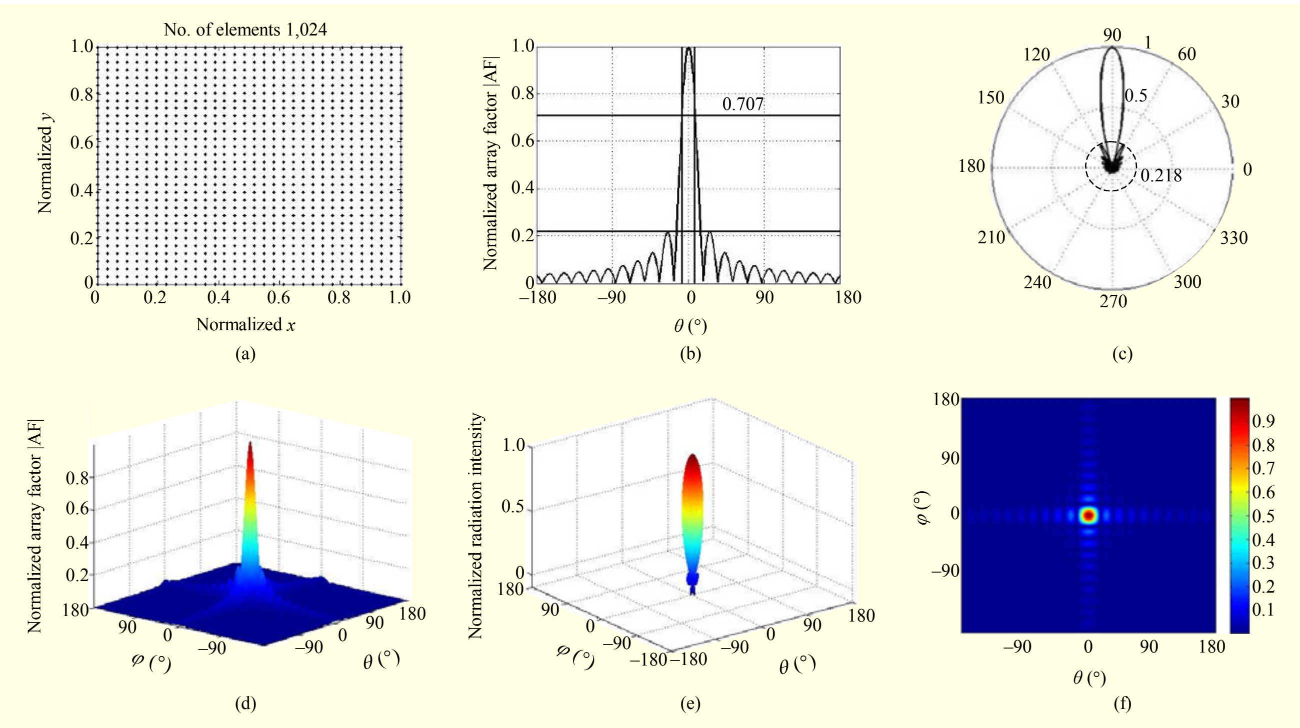


Fig. 3. Uniform antenna array: (a) shape, (b) array factor in Cartesian, (c) array factor in polar, (d) array factor in 3D Cartesian, (e) array factor in 3D spherical, and (f) array factor in Cartesian top view.

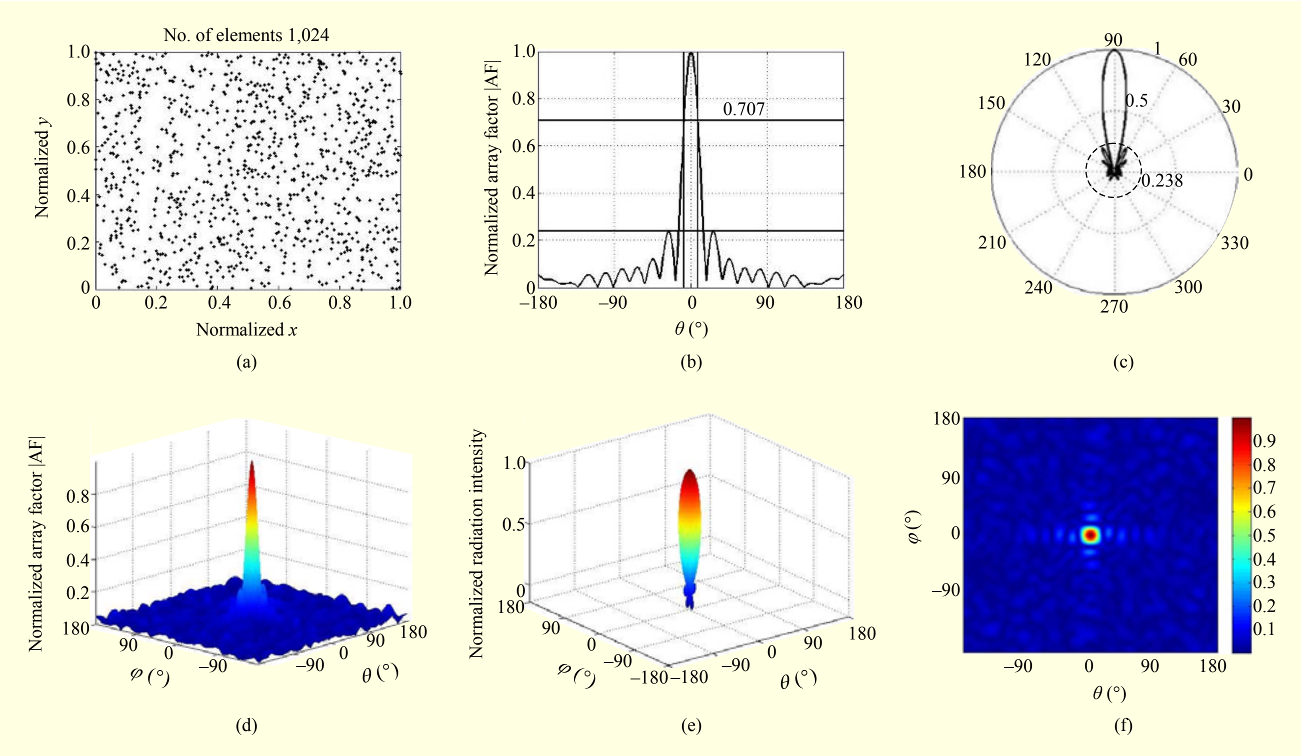


Fig. 4. Random antenna array: (a) shape, (b) array factor in Cartesian, (c) array factor in polar, (d) array factor in 3D Cartesian, (e) array factor in 3D spherical, and (f) array factor in Cartesian top view.

we can reformulate (6) to be in Cartesian coordinates as follows [23]. For the inter-elements distances on the $x$, $y$ axes, we have

$$dx = k\sin(\theta)\cos(\varphi) \text{ and } dy = k\sin(\theta)\sin(\varphi), \quad (12)$$

$$AF(x,y) = \sum_{N,M} I_n(x_n, y_n)\exp\left[j(dx\cdot x_n + dy\cdot y_n)\right]. \quad (13)$$

The general form for AF which is given by (13) can be used for any array geometry.

The array will be assumed to have 1,024 elements [26]-[31]; hence, the distributions will be as follows (fractal generators are given in the appendix). For the UAA, the response is shown in Fig. 3 with ($N$=32 and $M$=32)

The elements can be distributed randomly forming RAA as shown in Fig. 4.

The Sierpinski equilateral gasket antenna array is shown in Fig. 5 with its AF. The number of elements is 729 for 6 iterations, which is the closest number to 1,024. As for 7 iterations, the number of elements would be 2,187, which is far greater than1,024.

The first proposed array is the Dragon fractal array. The number of elements is 729 for 6 iterations. As for 7 iterations, the number of elements also would be 2,187. The array and its AF is shown in Fig. 6. This array exhibits the lowest SLL, about 0.07, of the proposed arrays in this research.

The second proposed array is the Flap fractal array. It has a wide angle seperating the main lobe from the side lobe. The number of elements is 1,024 using 5 iterations. The angle between the main and the side lobe is about 58º. The array and its response are shown in Fig. 7

The last proposed array is the Twig array, which combines the features of the Dragon and the Flap arrays. It has a low SLL with a very wide angle seperating the side lobe from the main lobe. The number of elements is 1,024, which can be produced using 6 iterations. The array and its AF is shown in Fig. 8.

The arrays responses are summerized in Table 1.

## V. Conclusion

In this work, we have demonstrated that the FAAs are attractive replacements for the UAAs or the RAAs. They have multifrquency tuninng, and they are space compact so they require no further space to add extra elements like UAAs and RAAs. The three proposed arrays show a superior performance compared to the commonly used Sierpinski FAA. This superiority comes from the high concentration of elements. This concentration gave these arrays a low SLL or a wide seperation angle between the SLL and ML. This concentration should not exceed certain limit otherwise the benefits of the array will be lost and the behavior of the

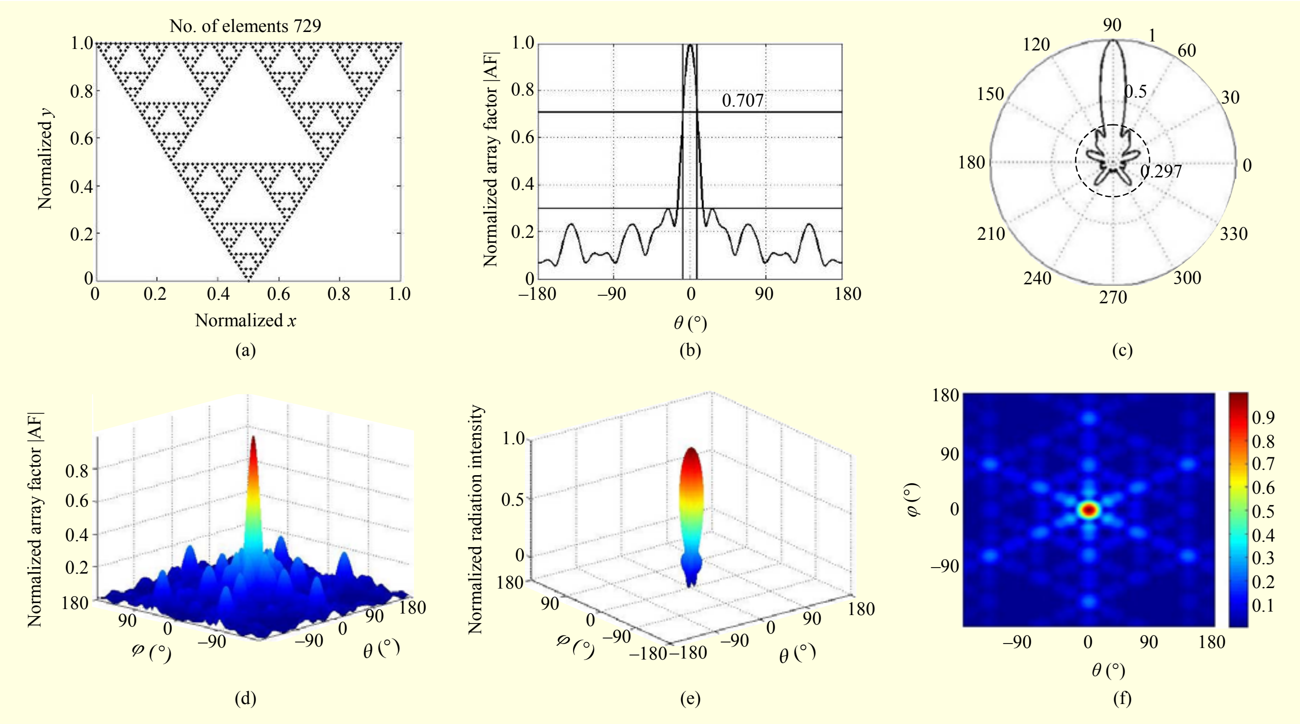


Fig. 5. Sierpinski equilateral gasket antenna array: (a) shape, (b) array factor in Cartesian, (c) array factor in polar, (d) array factor in 3D Cartesian, (e) array factor in 3D spherical, and (f) array factor in Cartesian top view.

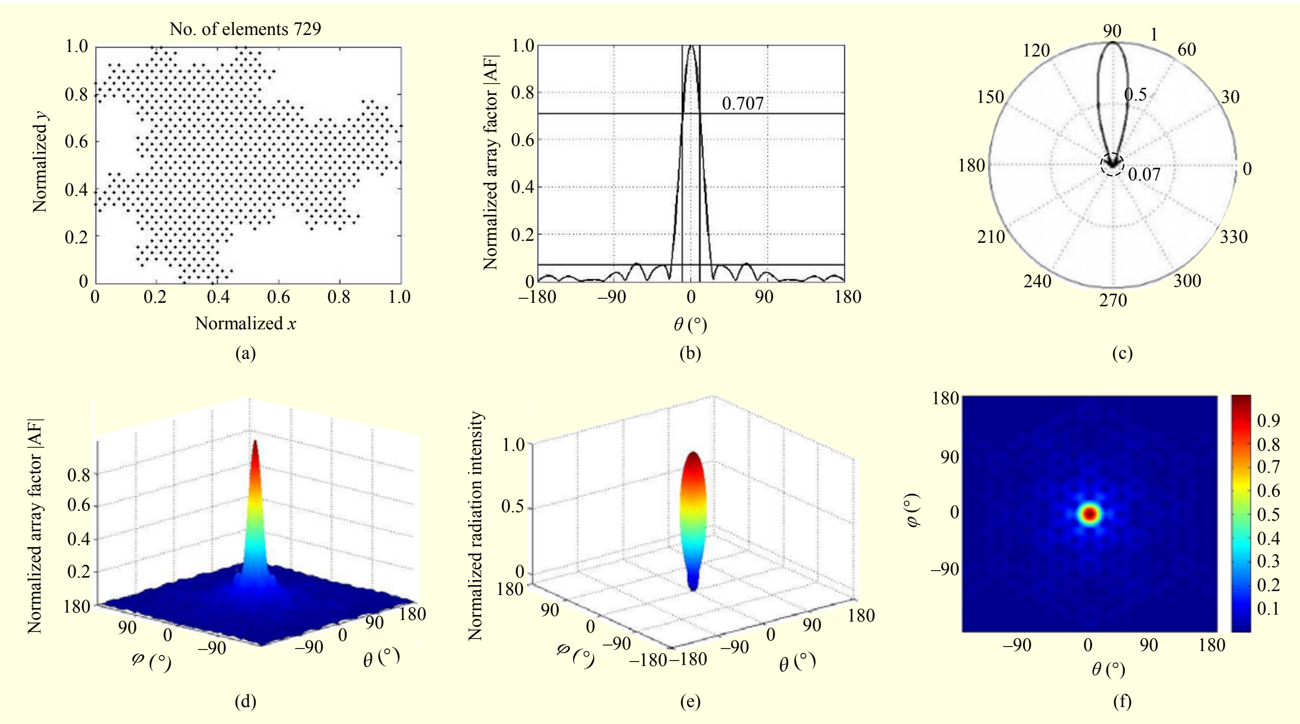


Fig. 6. Dragon fractal antenna array: (a) shape, (b) array factor in Cartesian, (c) array factor in polar, (d) array factor in 3D Cartesian, (e) array factor in 3D spherical, and (f) array factor in Cartesian top view.

aggregate would look like a single element. The reduction in SLL comes on the expense of widening the ML. Dragon requires more space than Sierpinski, while the Twig array requires the least area among all of them. Hence, Twig is

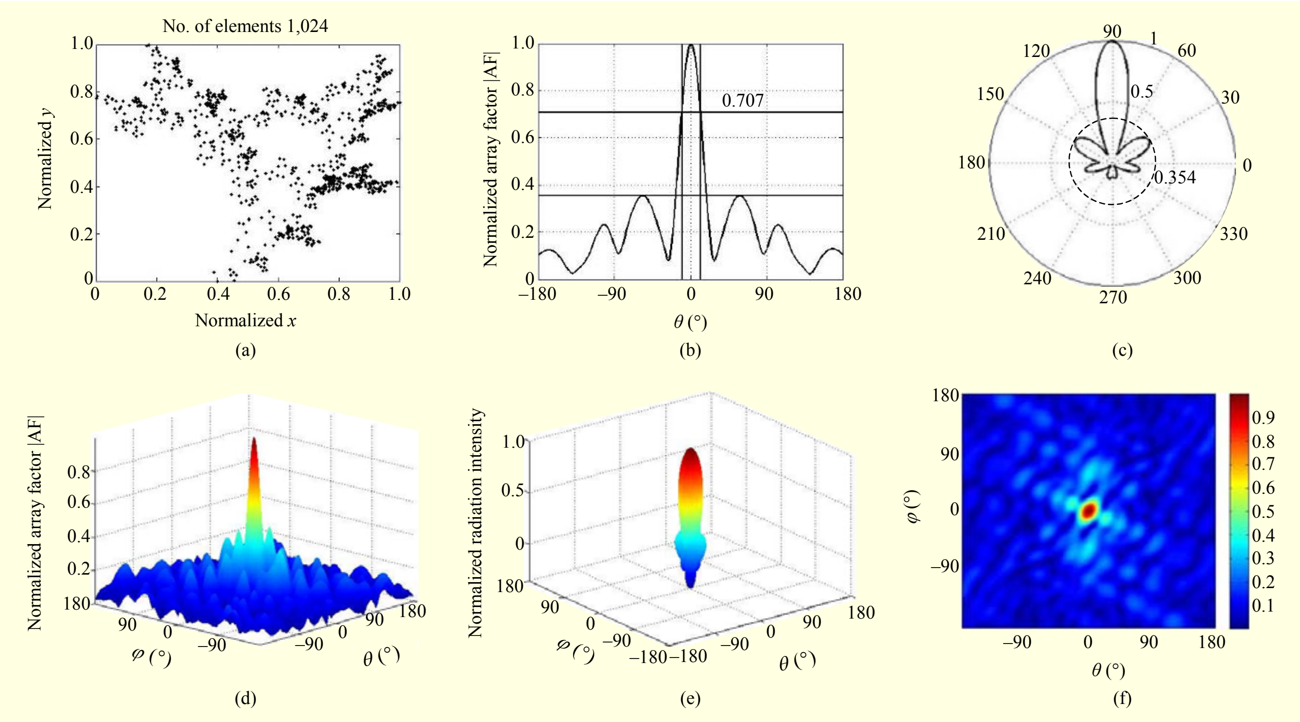


Fig. 7. Flap fractal antenna array: (a) shape, (b) array factor in Cartesian, (c) array factor in polar, (d) array factor in 3D Cartesian, (e) array factor in 3D spherical, and (f) array factor in Cartesian top view.

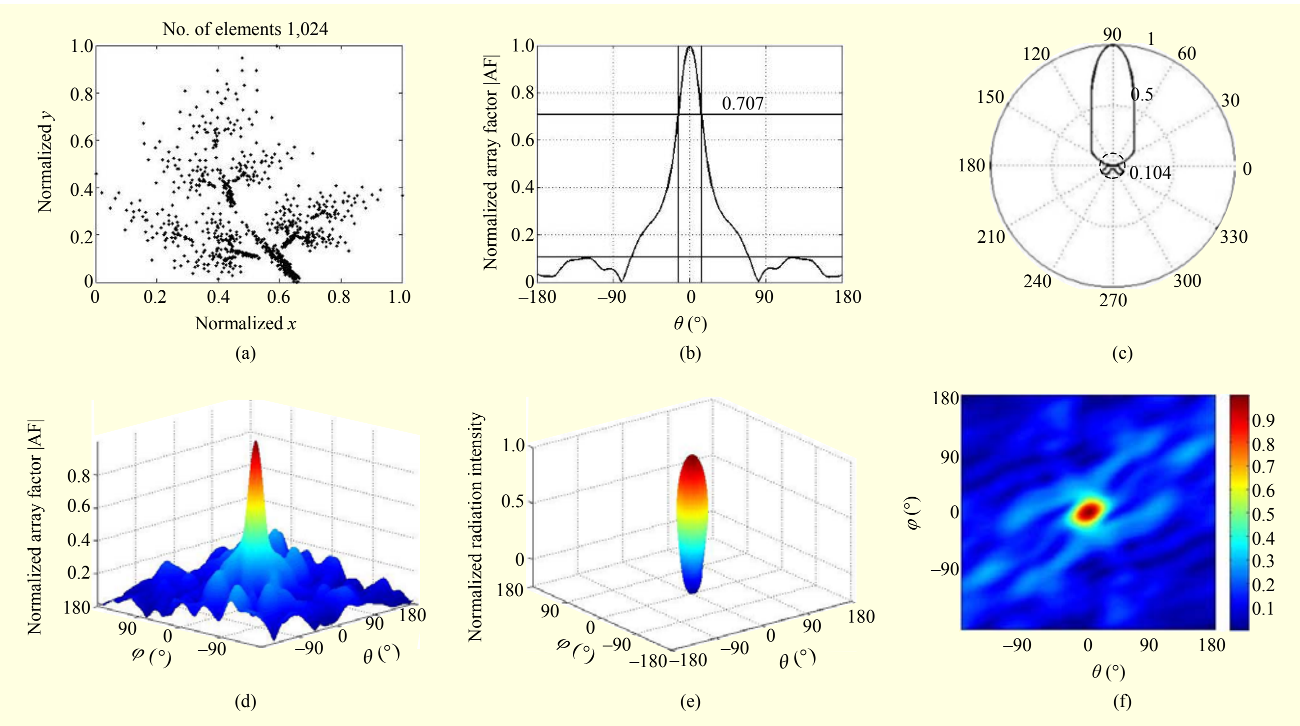


Fig. 8. Twig fractal antenna array: (a) shape, (b) array factor in Cartesian, (c) array factor in polar, (d) array factor in 3D Cartesian, (e) array factor in 3D spherical, and (f) array factor in Cartesian top view.

adequate for applications that are space limited, such as satellites, galactic surveillance, and space stations.

We intend to further investigate other fractal shapes that may show other interesting performance.

Table 1. Comparison of array factor properties for antenna arrays.

| Array Topology | ML* beam width | SLL | SLL (dB) | SLL angle |
|---|---|---|---|---|
| UAA | 15.26° | 0.218 | –13.23 | 26° |
| RAA | 16.16° | 0.238 | –12.47 | 28° |
| Sierpinski | 17° | 0.297 | –10.55 | 26° |
| Dragon | 20.65° | 0.07 | –23.1 | 34° |
| Flap | 21.55° | 0.354 | –9.02 | 58° |
| Twig | 26.93° | 0.104 | –19.66 | 125° |

*Main lobe

## Appendix

1. Sierpinski equilateral gasket

$$\Im_1\left(\left[\chi_1,\chi_2,1\right]\right)=\left[\chi_1,\chi_2,1\right]\begin{bmatrix}0.5 & 0 & 0\\ 0 & 0.5 & 0\\ 0.25 & 0 & 1\end{bmatrix}$$

$$\Im_2\left(\left[\chi_1,\chi_2,1\right]\right)=\left[\chi_1,\chi_2,1\right]\begin{bmatrix}0.5 & 0 & 0\\ 0 & 0.5 & 0\\ 0 & 0.5 & 1\end{bmatrix}$$

$$\Im_3\left(\left[\chi_1,\chi_2,1\right]\right)=\left[\chi_1,\chi_2,1\right]\begin{bmatrix}0.5 & 0 & 0\\ 0 & 0.5 & 0\\ 0.5 & 0.5 & 1\end{bmatrix}$$

2. Dragon fractal

$$\Im_1\left(\left[\chi_1,\chi_2,1\right]\right)=\left[\chi_1,\chi_2,1\right]\begin{bmatrix}0 & 0.577 & 0\\ -0.577 & 0 & 0\\ 0.0951 & 0.5893 & 1\end{bmatrix}$$

$$\Im_2\left(\left[\chi_1,\chi_2,1\right]\right)=\left[\chi_1,\chi_2,1\right]\begin{bmatrix}0 & 0.577 & 0\\ -0.577 & 0 & 0\\ 0.4413 & 0.7893 & 1\end{bmatrix}$$

$$\Im_3\left(\left[\chi_1,\chi_2,1\right]\right)=\left[\chi_1,\chi_2,1\right]\begin{bmatrix}0 & 0.577 & 0\\ -0.577 & 0 & 0\\ 0.0952 & 0.9893 & 1\end{bmatrix}$$

3. Flap fractal

$$\Im_1\left(\left[\chi_1,\chi_2,1\right]\right)=\left[\chi_1,\chi_2,1\right]\begin{bmatrix}0.2 & -0.5 & 0\\ 0.3 & 0.4 & 0\\ -0.4 & 0.4 & 1\end{bmatrix}$$

$$\Im_2\left(\left[\chi_1,\chi_2,1\right]\right)=\left[\chi_1,\chi_2,1\right]\begin{bmatrix}0.5 & -0.1 & 0\\ 0.2 & 0.4 & 0\\ 0.5 & 0.4 & 1\end{bmatrix}$$

$$\Im_3\left(\left[\chi_1,\chi_2,1\right]\right)=\left[\chi_1,\chi_2,1\right]\begin{bmatrix}0.5 & 0.2 & 0\\ -0.2 & 0.7 & 0\\ 0 & -0.3 & 1\end{bmatrix}$$

$$\Im_4\left(\left[\chi_1,\chi_2,1\right]\right)=\left[\chi_1,\chi_2,1\right]\begin{bmatrix}-0.1 & 0.3 & 0\\ 0.1 & 0.1 & 0\\ 0.6 & 0.1 & 1\end{bmatrix}$$

4. Twig fractal

$$\Im_1\left(\left[\chi_1,\chi_2,1\right]\right)=\left[\chi_1,\chi_2,1\right]\begin{bmatrix}0.2 & -0.5 & 0\\ 0.3 & 0.4 & 0\\ -0.5 & 0.4 & 1\end{bmatrix}$$

$$\Im_2\left(\left[\chi_1,\chi_2,1\right]\right)=\left[\chi_1,\chi_2,1\right]\begin{bmatrix}0.2 & 0.4 & 0\\ -0.3 & 0.2 & 0\\ 0.4 & -0.4 & 1\end{bmatrix}$$

$$\Im_3\left(\left[\chi_1,\chi_2,1\right]\right)=\left[\chi_1,\chi_2,1\right]\begin{bmatrix}0.6 & 0.2 & 0\\ -0.1 & 0.7 & 0\\ -0.1 & 0.3 & 1\end{bmatrix}$$

$$\Im_4\left(\left[\chi_1,\chi_2,1\right]\right)=\left[\chi_1,\chi_2,1\right]\begin{bmatrix}0 & -0.2 & 0\\ 0.1 & 0.3 & 0\\ 0 & -0.6 & 1\end{bmatrix}$$

## References


[1] M.-S. Lee, "A Low-Complexity Planar Antenna Array for Wireless Communication Applications: Robust Source Localization in Impulsive Noise," *ETRI J.*, vol. 32, no. 6, Dec. 2010, pp. 837-842.

[2] S. Lee and J. Thompson, "Simulation Models for Investigation of Multiuser Scheduling in MIMO Broadcast Channels." *ETRI J.*, vol. 30, no. 6, Dec. 2008, pp. 765-773.

[3] C. Sun et. al, *Handbook on Advancements in Smart Antenna Technologies for Wireless Networks*, Information Science Reference (an imprint of IGI Global), U. S., 2009.

[4] H. Cao et al., "Computationally Efficient 2-D DOA Estimation Using Two Parallel Uniform Linear Arrays," *ETRI J.*, vol. 31, no. 6, Dec. 2009, pp. 806-808.

[5] S. Pillai, K.-Y. Li, and B. Himed, *Space Based Radar Theory and Applications*, NY: McGraw Hill, 2008.

[6] R. Mailloux, *Phased Array Antenna Handbook*, 2nd ed., Artech

House Antennas and Propagation Library, 2005.
[7] G. Helmberg, *Getting Acquainted with Fractals*, KG, Berlin, Germany: Walter de Gruyter GmbH & Co., 2007.
[8] H.-O. Peitgen et al., *Chaos and Fractals New Frontiers of Science*, 2nd ed., NY: Springer Science and Business Media, Inc, 2004.
[9] D.H. Werner, R. Haupt, and P. Werner, "Fractal Antenna Engineering: the Theory and Design of Fractal Antenna Arrays," *IEEE Antenna Propag. Mag.*, vol. 41, no. 5, Oct. 1999, pp. 37-58.
[10] J. Gianvittorio, *Fractal Antennas: Design, Characterization, and Applications*, MSc Thesis, University of California, Los Angeles, 2000.
[11] J. Gianvittorio and Y. Rahmat-Samii, "Fractal Antennas: A Novel Antenna Miniaturization Technique, and Applications," *IEEE Antennas Propag. Mag.,* vol. 44, no. 1, Feb. 2000, pp. 20-36.
[12] D. Werner et al., "The Peano-Gosper Fractal Array," *IEEE Trans. Antennas Propag.*, vol. 51, no. 8, Aug. 2003, pp. 2063-2072.
[13] F. Bruno and C. Raga, *Simulation Algorithms for Fractal Radiation*, PhD Thesis, University of Missouri-Columbia, 2009.
[14] R. Hussein and F. Jibrael, "Comparison of the Radiation Pattern of Fractal and Conventional Linear Array Antenna," *Progress Electromagnetics Research Lett.*, vol. 4, 2008, pp. 183-190.
[15] H. Pan et al., "Array Analysis using High Efficiency Mm-wave Antenna for Gigabit Plus Throughput Wireless Communication," *Antennas Propag. Soc. Int. Symp.*, June 2009.
[16] M. Elhefnawy and W. Ismail, "A Microstrip Antenna Array for Indoor Wireless Dynamic Environments," *IEEE Trans. Antennas Propag.*, vol. 57, no. 12, Dec. 2009, pp. 3998-4002.
[17] E. Yaacoub and Z. Dawy, "On WCDMA Downlink Capacity with Power Allocation Strategy and Adaptive Antenna Arrays," *IEEE Commun. Soc. Subject Matter Experts for Publication ICC Proc.*, 2008.
[18] W. Aerts, *Application Specificities of Array Antennas: Satellite Communication and Electromagnetic Side Channel Analysis*, PhD Thesis, Katholieke Universiteit Leuven, Belgium, 2009.
[19] Q. Luo, H. Salgado, and J.-R. Pereira, "Printed Fractal Monopole Antenna Array for WLAN," *Int. Workshop Antenna Technol.*, 2010.
[20] K. Siakavara, "Hybrid-Fractal Direct Radiating Antenna Arrays with Small Number of Elements for Satellite Communications," *IEEE Trans. Antennas Propag.*, vol. 58, no. 6, 2010, pp. 2102-2106.
[21] A. Fenn, *Adaptive Antennas and Phased Arrays for Radar and Communications*, Massachusetts Institute of Technology, Lincoln Laboratory, Artech House, 2008.
[22] J. Sahalos, *Orthogonal Methods for Array Synthesis Theory and the ORAMA Computer Tool*, John Wiley and Sons, 2006.
[23] Y. Kim and D. Jaggard, "The Fractal Random Array," *Proc. IEEE*, vol. 74, no. 9, 1986, pp. 1278-1280.
[24] A. Bondarenko and Y. Mikhailova, "Radiation Pattern Synthesis for Arrays Based on Sierpinski Gasket," *9th Russian-Korean Int. Symp. Sci. Technol.*, 2005.
[25] S. Holm et al., "Properties of the Beampattern of Weight- and Layout-Optimized Sparse Arrays," *IEEE Trans. Ultrasonic, Ferroelect, Frequency Control*, vol. 44, no. 5, Sept. 1997, pp. 983-991.
[26] P. Hall, *The Square Kilometer Array: An Engineering Perspective*, Springer, 2005.
[27] J. Vaate et al, "First Celestial Measurement Results of the Thousand Element Array," *URSI GA,* Maastricht, Aug. 2002.
[28] E. Lera-Acedo et al., "System Noise Analysis of an Ultra Wide Band Aperature Array Element for Low Frequency Radio Astronomy," *Proc. 6th IASTED Int. Conf. Antennas, Radar, Wave Propag.*, 2009, track 649-024, pp. 118-123.
[29] G.W. Kant et al. "Receiver Architecture of the Thousand Element Array (THEA)," *Proc. SPIE*, vol. 4015, 2000.
[30] Astron, *Astron Annual Report*, Astron, 2009.
[31] Tom Oosterloo et al., "Apertif - The Focal-Plane Array System for the WSRT," *WideField Sci. Technol. SKA SKADS Conf.*, 2009.

**Ahmed Najah Jabbar** received the BSc and MSc in electronic and communication engineering from Al-Nahrain University, Baghdad, Iraq, in 1994 and 1997, respectively. From 1998 to 2000, he worked as the head of the Computer Science Department, Al-Zintan Higher Institute for Trainers Preparation, Libya. From 2002 to 2005, he worked as a teacher at the Department of Electronic and Communication Engineering, Hadhramout University of Technology, Yemen. Since 2005, he has been teaching in the Electric Department, College of Engineering, University of Babylon, Iraq. His research interests include the simulation and analysis of antennas, antenna arrays, smart antenna arrays, and microwave devices.